Time-Resolved 3D Contrast-Enhanced MRA with 2D Homodyne and View Sharing for Contrast Bolus Dynamics of the Brain

C. R. Haider[1], H. H. Hu[1], A. J. Madhuranthakam[2], D. G. Kruger[1], N. G. Campeau[1], J. Huston 3rd[1], S. J. Riederer[1]

[1]Department of Radiology, Mayo Clinic College of Medicine, Rochester, MN, United States, [2]GE ASL East, Boston, MA, United States

INTRODUCTION In addition to morphological imaging of the neck and intracranial vasculature in 3D contrast-enhanced MR angiography (CE-MRA), functional imaging of the contrast bolus flow dynamics plays a key role in the diagnosis of vascular diseases. By capturing both arterial and venous contrast kinetics of the entire vasculature, 3D time-resolved (TR) techniques [1] can provide crucial information such as the duration of the contrast material within arteries of interest and the transit time between arterial and adjacent venous enhancement. This data can be subsequently used to prescribe an appropriate non-TR morphological acquisition that optimally matches k-space data filling with the contrast signal behavior. Recently, a modified elliptical centric (EC) view order was developed to improve speed and spatial resolution performance in morphological 3D CE-MRA [2]. It exploits 2D homodyne (HD) reconstruction by undersampling both k_Y-phase and k_Z-slice encoding directions simultaneously [3]. In this work, we hypothesize that the k-space sampling footprint of this modified EC view-order can be further extended to 3D TR imaging. Using an eight-channel head coil, we demonstrated the technique's feasibility in 4 volunteers. 3D TR-data sets of the neck and intracranial vasculature were acquired with a voxel size of 0.8×1.5×3.5 mm^3 and a frame rate 2.3 seconds per 3D volume.

METHODS Fig. 1 illustrates the k-space sampling strategy of the TR technique. In the k_Y-k_Z phase encoding plane, k-space is separated into two parts – a central ellipse (red) and an outer annulus consisting of alternating vanes (blue and black). Frequency encoding is perpendicular to the page and consists of full echoes. Data collection follows a reverse EC view-order. Fig. 1A shows views acquired after the first reconstruction frame. The red ellipse serves two purposes – (i) to capture contrast bolus dynamics with central k-space and (ii) to provide an estimate of phase across the imaging volume. The sampled blue and black vanes in the outer annulus are used to homodyne reconstruct non-sampled conjugate views that are asymmetric. In Fig. 1B, views in the red ellipse are re-acquired and replaced. Views in the outer annulus previously acquired in time point 1 are now denoted in black. Freshly acquired vanes for time point 2 are represented in blue, from which corresponding non-sampled conjugate views are reconstructed using HD. This process of updating the red ellipse, acquiring additional vanes, and reconstructing complementary conjugate views with HD continues through time point 3 (1C) and 4 (1D), upon which all views in k-space have either been truly-acquired or HD reconstructed. In time point 5 (not shown), the same view locations sampled in time point 1 are re-acquired, and the four-part cycle continues. A 3D HD reconstruction is performed after every time point, yielding a snapshot of the dynamic process being imaged.

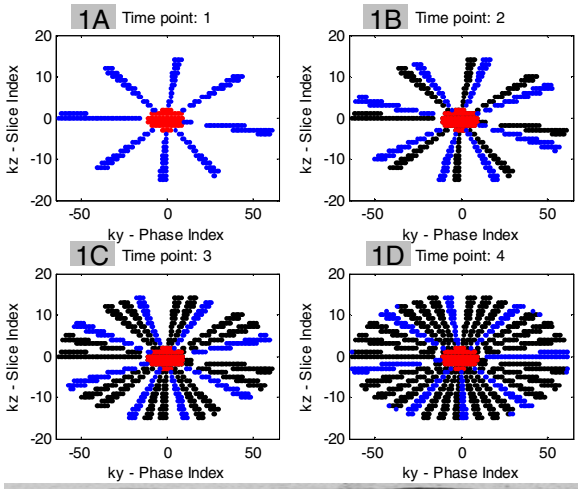

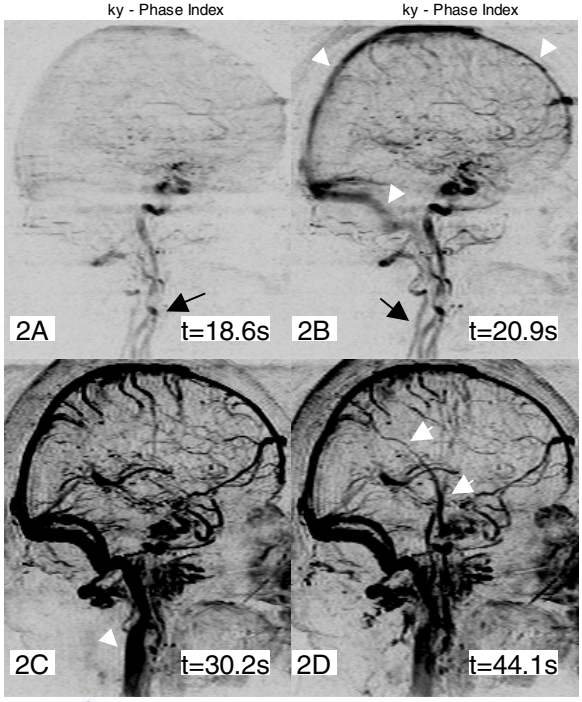

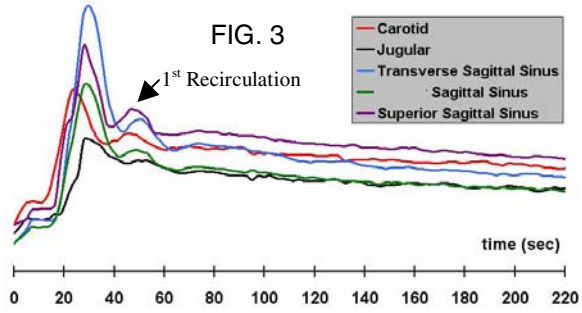

In Vivo Studies All volunteers were approved by our institution's review board. Examinations were preformed on a GE 1.5T Excite 11.0 scanner with an eight-element head coil. A 3D fast spoiled gradient echo sequence was used to acquire sagittal slices with the following parameters: repetition/echo time = 5-5.7/2.4 ms, flip angle 30°, FOV = 20-22 cm, BW = ±62.5 kHz, sampling matrix 256x128x32, with an associated voxel dimension of 0. 8×1.5×3.5-6 mm^3. Axes definitions were S/I–readout (X), A/P–phase (Y), and R/L–slice (Z). Each time-resolved acquisition lasted between 2-4 minutes, with a temporal frame resolution of 2.3 seconds. Ninteen ml of Gadolinium contrast was injected at 3 ml/s followed by 25 ml of saline at 2 ml/s. All data sets were reconstructed offline.

RESULTS Fig.2 (A-D) illustrates sagittal maximum intensity projections for a particular volunteer at 18.6, 20.9, 30.2, and 44.1 seconds after contrast injection. In 2A, initial filling of the carotid and vertebral arteries (arrow) can be seen. In 2B, 2.3 seconds after 2A, increased contrast enhancement in the carotid and vertebral arteries is noted (arrow). Note also that the large dural sinuses (white arrowheads), including the superior sagittal, transverse, and sigmoid sinuses are beginning to show enhancement as a result of venous return. In 2C, 30.2 seconds after contrast injection, the large dural sinuses are completely opacified, including several small cerebral vessels, and the jugular veins (white arrowhead). In 2D, additional venous drainage can be observed (white arrows). Fig 3 shows a contrast signal profile plot for five vessels using region-of-interest measurements from a different volunteer data set. First pass of the contrast bolus through the carotid arteries, the dural sinuses, and the jugular veins is clearly evident. A set of secondary signal peaks signifies the first recirculation (second pass) of the contrast bolus, approximately 20 seconds later. Contrast signals in all five vessels reach equilibrium after the second pass, and even after three minutes, continue to decrease slowly toward baseline value.

CONCLUSION We have demonstrated the feasibility of time-resolved imaging using a modified EC view-order that combines projection-like k-space sampling with view-sharing and homodyne reconstruction. While the spatial and temporal resolutions used in these preliminary studies are more appropriate for peripheral CE-MRA, further development of the technique is needed to achieve both faster (500 ms) temporal resolution and sub-millimeter spatial resolution for clinically useful application to the intracranial vasculature. One option to achieve this is incorporation of parallel imaging.

[1] Korosec F. MRM 1996;36:345-51. **[2]** Madhuranthakam AJ. Proc. 12th ISMRM Mtg, Kyoto, 2004;8. **[3]** Noll RC. IEEE TMI 1991;10:154:163.